Macromolecules **1995,** *28,* 6155–6160

Modification of Crystallization Properties of Poly(ethylene terephthalate) by Copolymerization with Arylate Units. 1. Preparation and Isothermal Crystallization of 4,4′-Biphenol-Containing Copolymers

Yoshimitsu Sakaguchi,* Masami Okamoto, and Itsuro Tanaka

Toyobo Research Center, Toyobo Company, Ltd., 1-1 Katata 2-Chome, Ohtsu 520-02, Japan

Received January 31, 1995; Revised Manuscript Received May 31, 1995[⊗]

ABSTRACT: Crystallization properties of the copolymers of poly(ethylene terephthalate) (PET) comprised of a small amount of 4,4′-biphenol units were compared by isothermal crystallization with the time-resolved light scattering method. These copolyesters were prepared from PET, terephthalic acid, and 4,4′-biphenol diacetate by acidolysis reaction and following polycondensation. The copolymer with 2 mol % of 4,4′-biphenol had a crystallization characteristic similar to that of PET with a decreased crystallization rate. On the other hand, the copolymers containing 4 and 8 mol % of 4,4′-biphenol showed enhanced crystal nucleation, and the 8 mol % copolymer had a crystallization rate of ca. twice as fast as that of PET. In these systems, wide-angle X-ray diffraction peaks of the crystal which appeared with crystallization were similar to those of PET, though another ordered domain was observed in the 8 mol % copolymer, which seems to have no direct influence on the crystallization and melting cycle.

Introduction

Poly(ethylene terephthalate) (PET) is used in various industrial fields such as fibers, films, bottles, and moldings. In the case of application as moldings, PET has a disadvantage of slow crystallization rate which is sometimes controlled by addition of crystal nucleation agents and/or plasticizers.[1–3] Although improvement of the crystallization rate of PET has been desired by many researchers, approach on the basis of copolymerization has been difficult to achieve. This is because the crystallizability usually decreases with an increase in the irregularity of the molecular structure. This paper, however, will describe that an arylate-unit-containing copolymer was found to show increased crystallizability compared to PET homopolymer.

Incorporation of a small amount of arylate units into PET was examined in order to modify the thermal properties of the homopolymer. Polyester synthesis with aromatic hydroxyl monomers by the usual ester exchange reaction, which is used for PET synthesis, is unfeasible because of a low nucleophilicity of aromatic hydroxyl groups. Therefore, an activated structure of the hydroxyl group, acetate, is employed to prepare whole aromatic polyesters and copolyesters of PET with aromatic comonomers: a representative example is poly(ethylene terephthalate-*co*-*p*-oxybenzoate) which is well-known as the first liquid crystalline polyester.[4] As this method is applicable to copolymerize PET with combinations of aromatic dicarboxylic acids and diols,[5] it is considered to be a preferable route to prepare a variety of structures of PET copolymers comprised of arylate units. In this study, a series of copolyesters derived from 4,4′-biphenol were prepared and their crystallizability was investigated.

Experimental Section

Materials. Poly(ethylene terephthalate) (Toyobo, RE530), 4,4′-biphenol (Tokyo Kasei Kogyo), terephthalic acid (Mitsui Petrochemical Ind.), acetic anhydride (Nacalai Tesque, GR), sulfuric acid (Nacalai Tesque, GR), and chlorobenzene (Nacalai Tesque, GR) were used without further purification.

Scheme 1

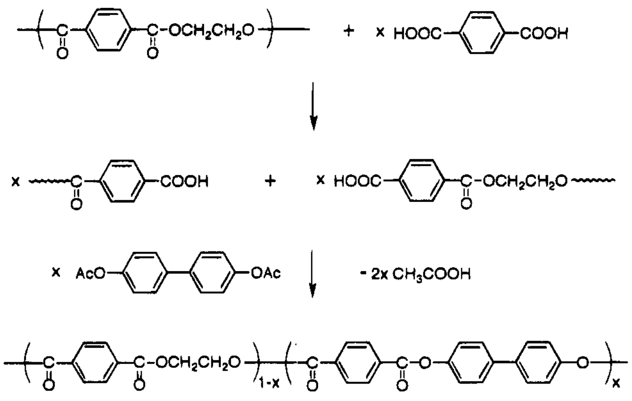

Preparation of 4,4′-Biphenol Diacetate.[6] 4,4′-Biphenol (122 g, 0.658 mol), acetic anhydride (450 mL), and sulfuric acid (1 mL) were stirred at 100 °C for 30 min. After cooling to room temperature, the reaction mixture was filtered. A white crystal collected was washed with 1 L of an aqueous 3% sodium hydroxide solution and pure water and then dried. Recrystallization was carried out by using toluene as a solvent. Yield: 90%. Mp: 167 °C.

Preparation of Copolymers. Copolymers were synthesized from PET and equimolar combinations of terephthalic acid and 4,4′-biphenol diacetate. In this reaction, acidolysis reaction of PET by the terephthalic acid occurs, and then polycondensation of the carboxylic chain ends and the 4,4′-biphenol diacetate proceeds as illustrated in Scheme 1.

As an example, preparation of the 4,4′-biphenol-containing copolymer with a feed ratio of 10 mol % is described. PET (19.2 g, 0.100 mol), terephthalic acid (1.83 g, 0.0110 mol), 4,4′-biphenol diacetate (2.97 g, 0.0110 mol), and 10 mL of chlorobenzene were placed in a glass vessel at 150 °C under a nitrogen flow. The mixture was heated to 280 °C and kept at that temperature for 30 min with stirring to proceed acidolysis reaction. Then, vacuum was applied gradually to reach 0.3 mmHg in 30 min, and the polymerization was continued for 3 h. Other copolymers were prepared by the same procedure except changing the comonomer feed ratio.

No catalyst was added for the copolymerization to minimize the influence of residual catalyst on the crystallization properties of the resultant copolymers. As a result, the copolymers as-polymerized showed relatively low solution viscosities (η_{sp}/C) around 0.3–0.4. Therefore, solid-state polymerization was

---

* To whom correspondence should be addressed.

[⊗] Abstract published in *Advance ACS Abstracts,* August 1, 1995.

0024-9297/95/2228-6155$09.00/0

Table 1. Preparation and Properties of TA–BP Copolymers

	monomer feed ratio		polymer composition[b]		DSC[d]				TGA (5%)[e]	
polymer[a]	TA (%)	BP (%)	BP (%)	η_{sp}/C[c] (dL/g)	T_g (°C)	T_{ch} (°C)	T_m (°C)	T_{cc} (°C)	in air (°C)	in N_2 (°C)
PET	0	0	0	0.84	81	148	257	208	352	402
TA–BP-2	2	2	2	0.93	82	149	250	189	355	404
TA–BP-4	5	5	4	1.03	84	128	249	193	370	408
TA–BP-8	10	10	8	0.99	84	117	247	206	363	401

[a] Copolymers were solid state polymerized and then quenched from the melt. [b] Molar content of the 4,4′-biphenol unit determined by ^{1}H-NMR. [c] Reduced viscosity measured at a concentration of 0.4 g/dL in *p*-chlorophenol/1,1,2,2-tetrachloroethane (3/1). [d] Measured at a heating rate of 20 °C/min and a cooling rate of 10 °C/min in nitrogen. T_{ch}: crystallization temperature with heating from the glass. T_{cc}: crystallization temperature with cooling from the melt. [e] 5% weight loss temperature determined at a heating rate of 10 °C/min.

Table 2. Sequence Distributions in TA–BP-8

	proportion of signals			composition						
polymer	EG–TA–EG	EG–TA–BP	BP–TA–BP	EG	BP	P_{EG-BP}[a]	P_{BP-EG}[b]	$\bar{L}_{n,EG}$[c]	$\bar{L}_{n,BP}$[d]	B[e]
as-polymerized	0.836	0.159	0.005	0.915	0.085	0.087	0.935	11.5	1.1	1.02
after SSP	0.850	0.144	0.006	0.922	0.078	0.078	0.923	12.8	1.1	1.00

[a] Probability of finding a BP unit next to an EG unit given by EG–TA–BP/2EG. [b] Probability of finding an EG unit next to a BP unit given by EG–TA–BP/2BP. [c] Number-average sequence length of EG unit given by $1/P_{EG-BP}$. [d] Number-average sequence length of BP unit given by $1/P_{BP-EG}$. [e] Degree of randomness given by $P_{EG-BP} + P_{BP-EG}$.

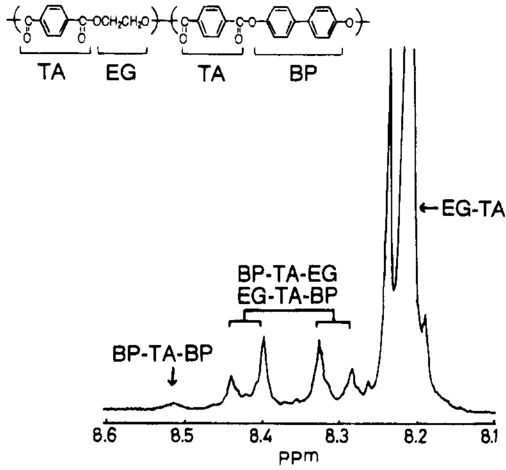

Figure 1. ^{1}H-NMR spectrum in the terephthaloyl region of TA–BP-8 after solid-state polymerization.

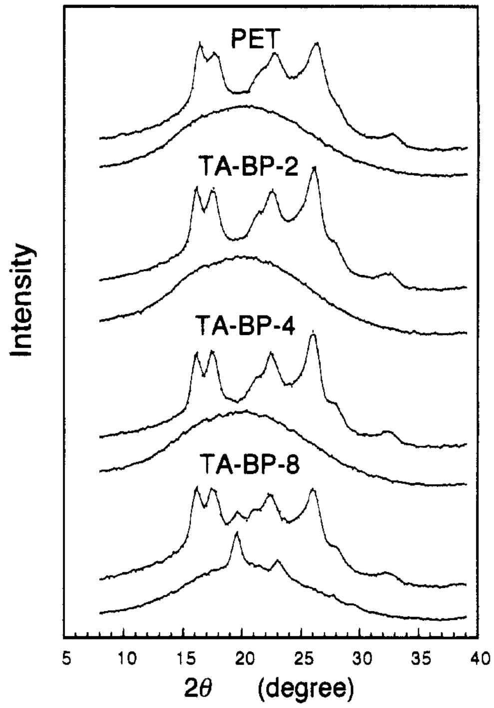

Figure 2. Wide-angle X-ray diffractograms of crystallized and quenched samples for PET and TA–BP copolymers.

carried out at 240 °C under vacuum for 15 h to increase their molecular weights up to the same level of η_{sp}/C as the original PET.

As a small amount of the comonomers sublimed during the copolymerization, each copolymer contained slightly less comonomers compared to the feed ratio. When the copolymerization was carried out below 10 mol % comonomer feed ratio, the polymerization proceeded as a homogeneous and transparent melt. On the other hand, the feed ratio of more than 10 mol % resulted in the appearance of turbidity of the polymer melt, and a further increase in the feed ratio such as 20 mol % caused solidification during the polymerization. Table 1 summarizes the results of preparation of three copolymers with monomer feed ratio below 10 mol %: they are abbreviated as TA–BP-2, TA–BP-4, and TA–BP-8 by using the content of the 4,4′-biphenol unit in the copolymers determined by ^{1}H NMR.

Figure 1 shows the ^{1}H-NMR spectrum of TA–BP-8 in the terephthaloyl region. There are three types of signals for terephthalate protons distinguished by the monomer unit sequence: a singlet for BP–TA–BP, a quartet for EG–TA–BP or BP–TA–EG, and signals for EG–TA–EG which split by probably an influence of longer sequences. Based on the integral values of these peaks, the sequence distribution can be evaluated according to the treatment of Yamadera and Murano.[8] Table 2 shows the results of calculation for the TA–BP-8 before and after the solid-state polymerization (the calculations used are expressed in the table). The number-average sequence lengths showed that the biphenylene terephthalate unit did not form consecutive blocks. Both of the polymers also showed the degree of randomness (B) around 1; as defined in Table 2, $B = 1$ when the distribution is random, and B decreases with an increase in the block length, and finally $B = 0$ for a homopolymer mixture. Therefore, these copolymers were considered as random copolymers.

Characterization. Reduced viscosities were measured at a concentration of 0.4 g/dL in a mixed solvent of *p*-chlorophenol and 1,1,2,2-tetrachloroethane (3/1, v/v) at 30 °C. ^{1}H-NMR spectra were obtained in a mixed solvent of dichloromethane-d_2 and deuterated trifluoroacetic acid with a Varian Gemini-200 spectrometer. Thermal transition temperatures were determined by using a differential scanning calorimeter (DSC) (Seiko DSC-20) at a heating rate of 20 °C/min and a cooling rate of 10 °C/min under flowing nitrogen for quenched samples from the melt. Thermogravimetric analysis (TGA) was conducted at a heating rate of 10 °C/min under flowing air or nitrogen, using a thermogravimetric analyzer (Shimadzu TGA-50). Wide-angle X-ray diffraction (WAXD) was conducted on a Rigaku rotating-anode generator (RV-200) with Nickel-

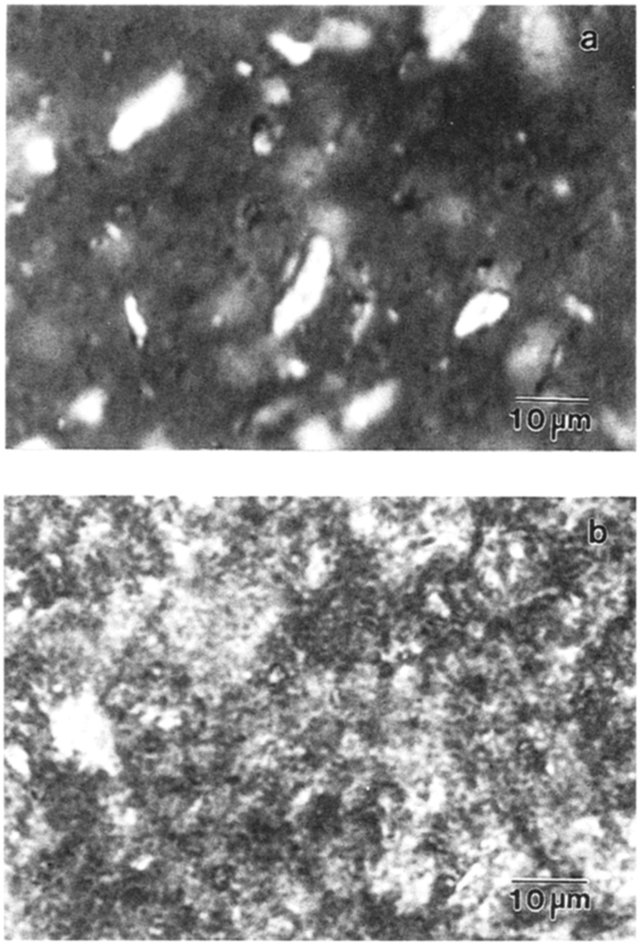

Figure 3. Polarized microscopic observation for TA−BP-8: (a) in the melt state at 300 °C; (b) after crystallization with cooling.

filtered Cu Kα radiation (40 kV, 100 mA) and a scintillation counter. Optical microscopic observation was carried out on a Nikon Type OPTIPHOT2-POL polarized-light transmission microscope.

Isothermal Crystallization with Time-Resolved Light Scattering. Time-resolved light scattering was carried out with a light scattering apparatus similar to that described in literature.[7] A sample was kept at 300 °C for 2 min between two pieces of cover glass to form a completely melted film (thickness: ca. 30 μm) and quickly transferred onto a hot stage (Linkam TH-600PH) of the light scattering apparatus set at a crystallization temperature. Change of the angular distribution of scattering intensity at an azimuthal angle of 45° under cross-polarized (H_V) optical alignment with time was recorded.

Results and Discussion

Crystalline Structure of Copolymers. Wide-angle X-ray diffraction was measured to study the crystalline structure of the copolymers. TA−BP-2 and TA−BP-4 showed the same diffraction pattern as that of PET with peaks at 2θ = 16.2, 17.8, 22.5, and 26.1° (Figure 2). Although it cannot be concluded by these data only that biphenylene terephthalate segments were segregated from the crystal domain, it is confirmed that the crystal consisted mainly of ethylene terephthalate segments. These polymers showed isotropic melt, and totally amorphous samples were obtained by quenching the melt samples with liquid nitrogen.

In TA−BP-8, on the other hand, extra peaks at 2θ = 19.7 and 23.3° were observed, and these peaks did not disappear by quenching from the melt state (Figure 2). Optical microscopic observation also showed remaining birefringence in the melt state as shown in Figure 3a. (The polymerization of TA−BP-8 proceeded as a homogeneous melt. These domains were observed after solid-state polymerization.) Although the usual DSC measurement for a solid-state polymerized TA−BP-8 showed only one T_m at 270 °C, a nominal heating rate of 200 °C/min gave another endothermic peak at 448 °C before thermal decomposition in addition to the peak of 294 °C that was shifted from 270 °C (Figure 4). These suggest the existence of a high melting point crystal which may be related to biphenylene-containing segments. As a 4,4′-biphenol unit exists randomly in the polymer chain, the structure of this ordered state is not clear at this stage.

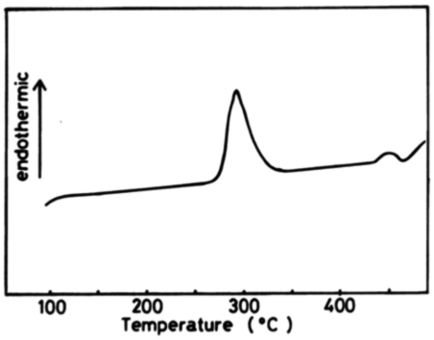

Figure 4. DSC curve for TA−BP-8 at a nominal heating rate of 200 °C/min.

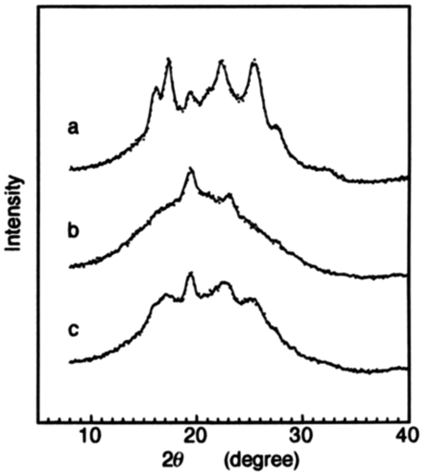

Figure 5. X-ray diffraction patterns of TA−BP-8: (a) cooled slowly from 300 °C; (b) quenched from 300 °C; (c) quenched samples heated up to T_{ch}.

Although the ordered domains which have high melting points exist in TA−BP-8, the diffraction peaks which appeared with the crystallization were similar to those of PET as found in TA−BP-2 and TA−BP-4 (Figure 5). Microscopic observation also showed that crystal nucleation occurred randomly in the melt, not from the surface of the high melting point crystal (Figure 3b). These ordered domains which have high melting points seem to have no direct influence on the crystallizing and melting behavior of TA−BP-8.

Isothermal Crystallization with Time-Resolved Light Scattering. Isothermal crystallization from the melt was carried out for the four polymers at various crystallization temperatures. Figure 6 shows the time dependence of a H_V light scattering profile for the polymers at a representative crystallization temperature, respectively. It also shows polarized microscopic photographs at the same crystallization temperatures.

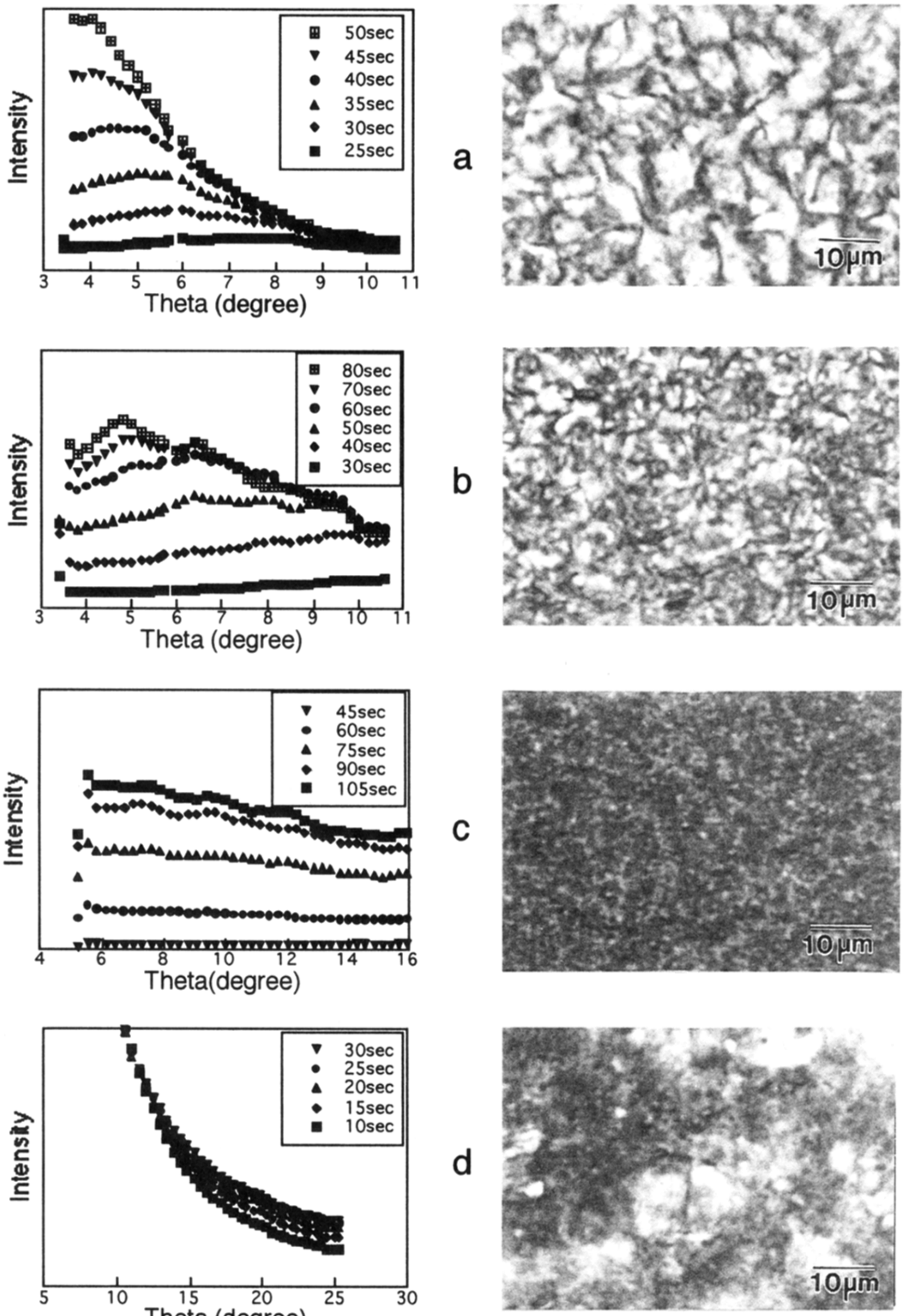

Figure 6. Time dependence of the light scattering profile and final polarized microscopic observation for PET and TA–BP copolymers under isothermal crystallization: (a) PET at 200 °C; (b) TA–BP-2 at 182 °C; (c) TA–BP-4 at 185 °C; (d) TA–BP-8 at 194 °C.

In the case of PET as seen in Figure 6a, there was a scattering peak, which shifted to lower angle with time. This means the spherulite growth. When the crystallization was performed at higher temperature, growth of a larger spherulite was observed; the scattering peak existed at lower angle, and also larger spherulites were directly detected on the microscopic observation.

TA–BP-2 showed a similar tendency to PET as illustrated in Figure 6b, though the sizes of the spherulites were a little smaller and the shapes were deformed to some extent.

The scattering profile of TA–BP-4 showed no apparent peak, and the scattering intensity increased similarly at any angle with time (Figure 6c). It is considered that size and shape of the spherulites were irregular in this system, and the randomness of optical anisotropy increased. The existence of small spherulites with diameter around 2 μm was detected from the microscopic photographs, and the nucleation density was much higher than that of PET and TA–BP-2. Apparent dependence of the crystallization temperature on the scattering profile was not observed.

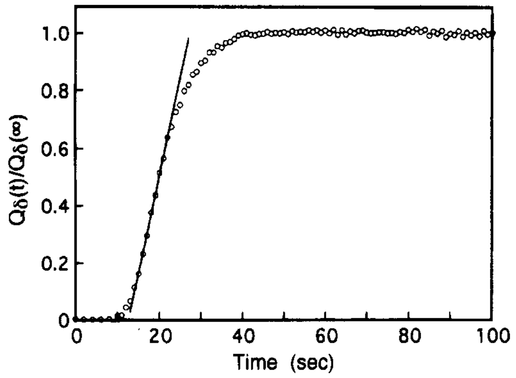

Figure 7. Time variation of invariant Q_δ for PET under isothermal crystallization at 180 °C.

As TA–BP-8 had the ordered phase even in the melt state, intense scatterings were observed at the low-angle region from the beginning of the crystallization (Figure 6d). When the crystallization proceeded, a slight increase in the intensity was measured, especially at higher angles. Although the increase of the scattering intensity was small, the degree of crystallinity achieved by the crystallization was about 70–80% of that of PET, which was ascertained by the heat of crystallization under isothermal crystallization with DSC. The microscopic photographs of TA–BP-8 showed the appearance of small crystals, which seem as spherulites with a size similar to those of TA–BP-4, from the amorphous region.

Invariant Q_δ of the scattering intensity for H_V (I_{H_V}) is defined as eq 1[9] and has a relation expressed by eq 2,

$$Q_\delta = \int I_{H_V} q^2 \, dq \tag{1}$$

$$Q_\delta \propto \langle \delta^2 \rangle = \phi_c(\alpha_1 - \alpha_2)^2 \tag{2}$$

where q is the magnitude of the scattering vector, $\langle \delta^2 \rangle$ is the mean-square anisotropy, ϕ_c is the volume fraction of the crystalline domain, and α_1 and α_2 are the principal polarizabilities of the crystal lamella. Here, ϕ_c at time t is given by eq 3,

$$\phi_c(t) = Q_\delta(t)/Q_\delta(\infty) \tag{3}$$

where $Q_\delta(\infty)$ is the attainable crystallinity in the crystalline domain at a given crystallization condition. From these relations, information on the crystallization kinetics in terms of ϕ_c can be obtained from the time variation of Q_δ. Figure 7 shows the change of Q_δ for PET with time at 180 °C as an example. Q_δ increased gradually with time after a certain induction time (t_0).

The overall crystallization rate was determined from the slope of $Q_\delta(t)/Q_\delta(\infty)$ (dQ/dt) in the crystallizing region as shown in Figure 7. Figure 8 compares the overall crystallization rates of the four polymers at various crystallization temperatures. The crystallization rate of TA–BP-2 was smaller than that of PET in the whole range of crystallization temperatures due to probably the reduction of regularity in the chain sequence induced by the biphenylene terephthalate unit. On the other hand, TA–BP-4 had a maximum of dQ/dt similar to that of PET, though the chain sequence was more irregular. The maximum temperature of dQ/dt for TA–BP-4 was lower than that of PET by ca. 15 °C. Moreover, TA–BP-8 showed the maximum of dQ/dt to be about twice as large as that of PET. In spite of the increase in chain irregularity, an increase in the content of the biphenylene terephthalate unit has some effect to accelerate the crystallization of the copolymers.

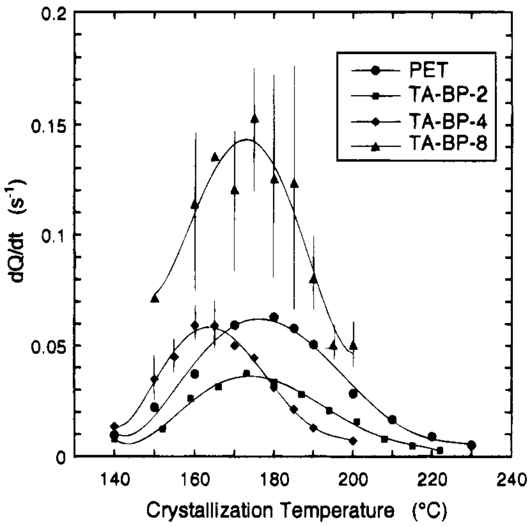

Figure 8. Temperature dependence of the overall crystallization rate for PET and TA–BP copolymers under isothermal crystallization.

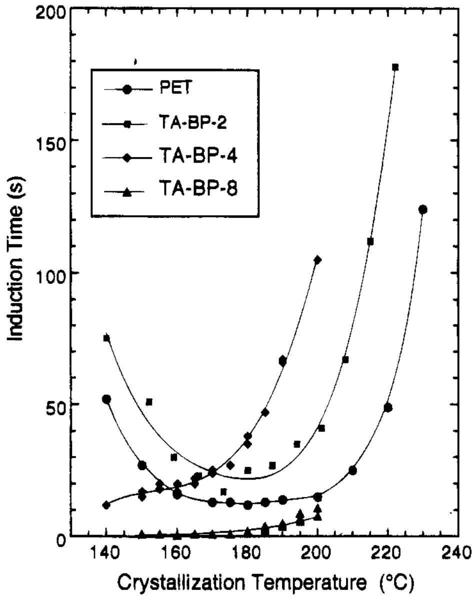

Figure 9. Temperature dependence of the induction of time of PET and TA–BP copolymers under isothermal conditions.

Changes in the induction time with crystallization temperature are illustrated in Figure 9. As a whole, an inverse relation was observed between the induction time and the crystallization rate. TA–BP-4 at lower crystallization temperature and TA–BP-8 in the whole range of crystallization temperatures showed remarkably short induction time. These results suggest that the existence of the biphenylene terephthalate unit has some contribution to enhance the nucleation.

Crystallization kinetics for polymers has been approximately described by the Avrami equation[10],

$$\phi_c = 1 - \exp(-k(t - t_0)^n) \tag{4}$$

where k is the rate constant and n is the Avrami index related to the geometry and mode of crystal growth. The equation for the Avrami plot is obtained from eqs 3 and 4.

$$\ln(-\ln(1 - Q_\delta(t)/Q_\delta(\infty))) = \ln k + n \ln(t - t_0) \tag{5}$$

The kinetic parameters are obtained by plotting the data

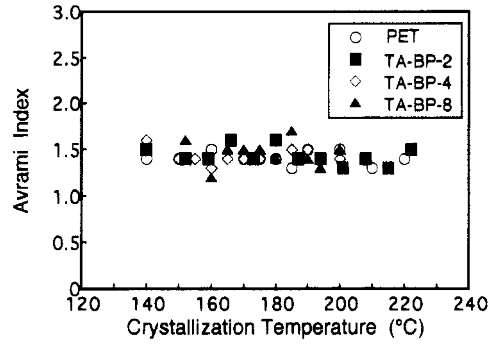

Figure 10. Temperature dependence of the Avrami index for PET and TA–BP copolymers.

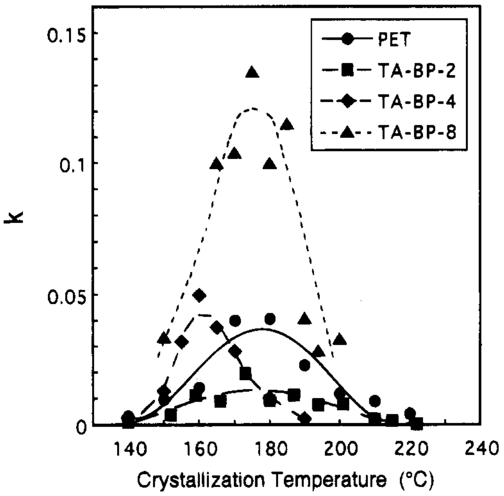

Figure 11. Temperature dependence of the crystallization rate (k) derived from Avrami treatment for PET and TA–BP copolymers.

according to eq 5; the slope is equal to n, and the intercept is equal to ln k.

Figure 10 shows the Avrami index obtained for the polymers. Almost constant n values around 1.5 were obtained for each polymer independent of crystallization temperatures. These results mean the crystallization mechanism for these polymers was the same. Although $n = 1.5$ is smaller than the values reported for PET, $n = 2.5-3.0$,[3,11,12] this is attributed to the selection of $t - t_0$ as the measuring time instead of t.

The rate constants (k) obtained by Avrami analysis are illustrated in Figure 11. Dependence of k on the polymer structure and crystallization temperature was consistent with that of the overall crystallization rate determined from dQ/dt.

One of the reasons of the increased crystallization rate in the 4,4′-biphenol-containing copolymers is attributed to the accelerated nucleation: this is supported by the increased nucleation density observed on polarized microscopy and the extremely reduced induction time with the isothermal crystallization in TA–BP-8. This effect is also found in the crystallization of TA–BP-4 below 165 °C in which the overall crystallization rate of TA–BP-4 was higher than PET. In this temperature region, the induction time of TA–BP-4 was smaller than that of PET and decreased with crystallization temperature in spite of the decrease of crystallization rate. This is considered as a result of accelerated nucleation induced by the existence of biphenylene terephthalate segments. As the biphenylene terephthalate content was relatively low in TA–BP-4, the accelerated nucleation may contribute to increase the overall crystallization rate only at lower temperature range in which the nucleation rate is dominant to determine the crystallization rate.

The mechanism for the effect of the biphenylene terephthalate unit on the accelerated nucleation is not clear at this moment. However, it is known that molecular orientation accelerates the crystallization of polymers. As one biphenylene terephthalate unit forms four consecutive *p*-phenylene moieties, this rigid portion in the polymer chain may contribute to a local orientation of the molecular chains on the molecular level.

Conclusion

Crystallization properties of PET copolymers comprising 2, 4, and 8 mol % of 4,4′-biphenol, TA–BP-2, TA–BP-4, and TA–BP-8 were compared with that of PET. In these systems, wide-angle X-ray diffraction peaks of the crystal which appeared with crystallization were similar to those of PET. In TA–BP-8, there was an additional ordered phase with a higher melting point, which seems to have no direct influence on the crystallization and melting cycle. TA–BP-2 showed spherulite growth similar to PET, though the crystallization rate was smaller. In the case of TA–BP-4 and TA–BP-8, increased nucleation density and appearance of smaller and irregular spherulites were observed. As a result, TA–BP-8 showed the maximum crystallization rate ca. twice as fast as that of PET for the isothermal crystallization.

References and Notes

(1) Berghmans, G. H.; Overbergh, N.; Smets, G. *J. Polym. Sci., Polym. Phys. Ed.* **1974**, *12*, 303.
(2) Mercier, J. P. *Polym. Eng. Sci.* **1990**, *30*, 270.
(3) Reinsch, V. E.; Rebenfeld, L. *J. Appl. Polym. Sci.* **1994**, *52*, 649.
(4) Jackson, W. J.; Kuhfuss, H. F. *J. Polym. Sci., Polym. Chem. Ed.* **1976**, *14*, 2043.
(5) Hamb, F. L. *J. Polym. Sci., Polym. Chem. Ed.* **1972**, *10*, 3217.
(6) Levine, M.; Temin, S. C. *J. Polym. Sci.* **1958**, *28*, 179.
(7) Okada, T.; Saito, H.; Inoue, T. *Macromolecules* **1992**, *25*, 1908.
(8) Yamadera, R.; Murano, M. *J. Polym. Sci., Polym. Chem. Ed.* **1967**, *5*, 2259.
(9) Koberstein, J.; Russell, T. P.; Stein, R. S. *J. Polym. Sci., Polym. Phys. Ed.* **1979**, *17*, 1719.
(10) Avrami, M. *J. Chem. Phys.* **1939**, *7*, 1103.
(11) Garcia, D. *J. Polym. Sci., Polym. Phys. Ed.* **1984**, *22*, 2063.
(12) Jabarin, S. A. *J. Appl. Polym. Sci.* **1987**, *34*, 85.

MA950111W